Simple Modeling of the AC Hysteretic Property of a Grain-Oriented Silicon Steel Sheet

Testuji Matsuo and Masaaki Shimasaki

Department of Electrical Engineering, Graduate School of Engineering, Kyoto University, Kyoto 615-8510, Japan

A homogenized model based on the Pry and Bean model is generalized to represent the ac hysteretic characteristics of an actual grain-oriented silicon steel sheet. A parameter for the frequency dependence of eddy-current loss is introduced. The generalized model improves the evaluation accuracy of eddy-current loss and the representation of ac B–H loops under the condition of a sinusoidal magnetic flux. The generalized model also accurately represents ac B–H loops having minor loops.

***Index Terms*—AC hysteresis, excess eddy-current loss, homogenization, Pry and Bean model.**

I. Introduction

RECENT developments in computer technology have enabled us to simulate detailed B and H fields in electrical machines. However, the accurate computation of B and H fields remains difficult because of the complex magnetic properties of silicon steel sheets including their excess (or anomalous) eddy-current loss [1]–[3], their hysteresis [3], and their vector property [4].

Grain-oriented silicon steel sheets are widely used as a core material, not only for transformers, but also for segmented core motors. Grain-oriented steel sheets have large excess eddy-current losses because they have larger magnetic domain sizes than nonoriented steel sheets [2].

Magnetic fields in motor cores have higher time harmonics because of their spatial harmonics and pulsewidth modulation (PWM) power control. Since higher time harmonics often cause complex minor hysteresis loops, the accurate representation of minor loops is required for detailed ac magnetic field analyses in motor cores.

On the other hand, several precise and efficient dc hysteresis models, such as play and stop models [5], [6] have been developed. For example, stop and play models having input-dependent shape functions [7], [8] have been applied to the accurate representations of the dc hysteretic characteristics of silicon steel sheets, including minor hysteresis loops [9].

A previous study [10] combines a dc hysteresis model and the Pry and Bean model [1] to derive a homogenized model for the ac characteristics of grain-oriented steel sheets. This homogenized model evaluates the excess eddy-current loss using an anomaly factor, which improves the representation of the ac hysteretic properties of a grain-oriented silicon steel sheet.

However, this homogenized model cannot achieve a sufficiently accurate representation of the ac properties because of its simplicity. This paper simply generalizes this ac hysteresis model to improve the accuracy of ac hysteretic representation.

Digital Object Identifier 10.1109/TMAG.2006.871636

II. AC Hysteresis Model

A. Simple Homogenized Model

Pry and Bean [1] have evaluated excess eddy-current losses assuming a one-dimensional (1-D) periodic magnetic domain structure. The Pry and Bean model gives the instantaneous eddy-current loss P_{E} per unit volume as

$$P_{\mathrm{E}} = k_{\mathrm{E}}(B)P_C \tag{1}$$

$$k_{\mathrm{E}}(B) = \frac{192L}{\pi^3 d} \times \sum_{n\mathrm{odd}}^{\infty} \frac{\cosh\left\{\frac{n\pi L}{d}\left(1+\frac{B}{B_{\mathrm{S}}}\right)\right\}\cosh\left\{\frac{n\pi L}{d}\left(1-\frac{B}{B_{\mathrm{S}}}\right)\right\}}{n^3 \sinh\frac{2n\pi L}{d}} \tag{2}$$

$$P_{\mathrm{C}} = \frac{\sigma d^2}{12}\left(\frac{\mathrm{d}B}{\mathrm{d}t}\right)^2 \tag{3}$$

where k_{E} is the anomaly factor, P_{C} is the classical eddy-current loss, σ is the electric conductivity, $2L$ is the average magnetic domain width, d is the sheet thickness, and B_{S} is the saturation magnetic flux density.

Reference [10] approximated $k_{\mathrm{E}}(B)$ as $k_{\mathrm{E}}(B) \approx k_{\mathrm{E}}(0)$, independently of B. The eddy-current loss P_{E} is factorized as

$$P_{\mathrm{E}} = H_{\mathrm{E}}\,\mathrm{d}B/\mathrm{d}t \tag{4}$$

$$H_{\mathrm{E}} = k_{\mathrm{E}}(0)\frac{\sigma d^2}{12}\frac{\mathrm{d}B}{\mathrm{d}t} \tag{5}$$

where H_{E} is the magnetic field caused by the eddy current. Accordingly, a simple homogenized model is derived as

$$H_{\mathrm{ac}}(t) = H_{\mathrm{dc}}(B(t)) + H_{\mathrm{E}}. \tag{6}$$

where H_{ac} is an applied ac magnetic field and $H_{\mathrm{dc}}(B)$ represents the dc hysteretic property.

B. Generalized Model

When the magnetic property of the steel sheet is linear, a sinusoidal magnetic field with frequency f yields an eddy-current loss per cycle W_{E} given as in [3]

$$W_{\mathrm{E}} = \begin{cases} \frac{\pi^2}{6}\sigma d^2 B_{\max}^2 f & (\text{for small } f) \\ \frac{\pi^{3/2}}{2}\sqrt{\frac{\sigma d^2}{\mu}} B_{\max}^2 f^{1/2} & (\text{for large } f) \end{cases} \tag{7}$$

where $B_{\max}$ is the amplitude of B.

Equation (7) implies that W_{E} is equal to the classical eddy-current loss for small f whereas it becomes proportional to $f^{1/2}$ for large f. This suggests that H_{E} becomes

$$H_{\mathrm{E}} \propto f^{1/2} \tag{8}$$

for a high-frequency eddy-current field.

On the other hand, the Pry and Bean model assumes that the magnetic domain walls are sufficiently rigid not to bow. If the magnetic domain walls are highly flexible and therefore allow the wall to bow freely, the eddy-current field in the steel sheet will satisfy (8) for large f because of the skin effect.

Actual steel sheets are neither perfectly flexible nor rigid; their eddy-current field is assumed to obey

$$\mathrm{W}_{\mathrm{E}} \propto f^{\gamma}, H_{\mathrm{E}} \propto f^{\gamma}, 0.5 \leq \gamma \leq 1. \tag{9}$$

Accordingly, H_{E} can be generalized as

$$H_{\mathrm{E}} = h_{\mathrm{EA}}\left(B, \frac{\mathrm{d}B}{\mathrm{d}t}\right) = c_{\mathrm{A}} k_{\mathrm{E}}(B) \frac{\sigma d^2}{12} \left(\frac{\mathrm{d}B}{\mathrm{d}t}\right)^{\gamma} \tag{10}$$

where c_{A} is a constant and the function $\mathrm{sign}(X)|X|^{\gamma}$ is simply denoted by X^{γ}.

Zirka *et al.* [11] proposed an ac hysteresis model that also has a more general form than (5) given by

$$H_{\mathrm{E}} = h_{\mathrm{EB}}\left(B, \frac{\mathrm{d}B}{\mathrm{d}t}\right) = c_{\mathrm{B}} \left(\frac{1}{1 - B^2/B_{\mathrm{S}}^2} \frac{\mathrm{d}B}{\mathrm{d}t}\right)^{\gamma} \tag{11}$$

where c_{B} is a constant.

An ac hysteresis model (5) using (10) or (11) is examined in this paper.

III. Simulation for Sinusoidal Magnetic Flux Density

AC B–H loops of a grain-oriented silicon steel sheet (JIS: 30P105) are simulated along its rolling direction. This steel sheet has an electric conductivity σ of 2×10^6 S/m. The one-dimensional magnetic properties of the steel sheet are measured using a single sheet tester [12] under the condition of a sinusoidal B. The simulated magnetic field H_{ac} is compared with the measured H where the measured B is given to calculate H_{dc} and H_{E}. The dc hysteretic property $H_{\mathrm{dc}}(B)$ is represented by the play model with an input-dependent shape function [8] identified from 20 symmetric B–H loops.

Fig. 1 shows the frequency dependence of the eddy-current loss of the steel sheet for five amplitudes of $B_{\max}$: 0.34, 0.68, 1.02, 1.36, and 1.70 T. The eddy-current loss per cycle W_{E} is given as

$$W_{\mathrm{E}} = \int_{\mathrm{cycle}} H_{\mathrm{ac}} \mathrm{d}B - \int_{\mathrm{cycle}} H_{\mathrm{dc}} \mathrm{d}B. \tag{12}$$

Fig. 1 shows that γ is almost constant at about 0.75.

This study compares three forms of the field H_{E} as follows:

$$H_{\mathrm{E}} = h_{\mathrm{EA}}(0, \mathrm{d}B/\mathrm{d}t), h_{\mathrm{EA}}(B, \mathrm{d}B/\mathrm{d}t), \text{and } h_{\mathrm{EB}}(B, \mathrm{d}B/\mathrm{d}t).$$

Parameter γ is set at 0.75 or 1.

Fig. 2(a) shows simulated B–H loops using $h_{\mathrm{EA}}(0, \mathrm{d}B/\mathrm{d}t)$ with $\gamma = 1$ at $f = 50$ and 400 Hz, where L/d is set at 0.9 to minimize the representation error at $f = 50$ Hz with $c_{\mathrm{A}} = 1$.

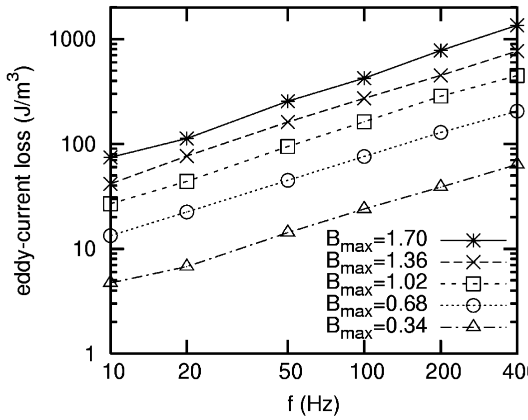

Fig. 1. Frequency dependence of eddy-current loss.

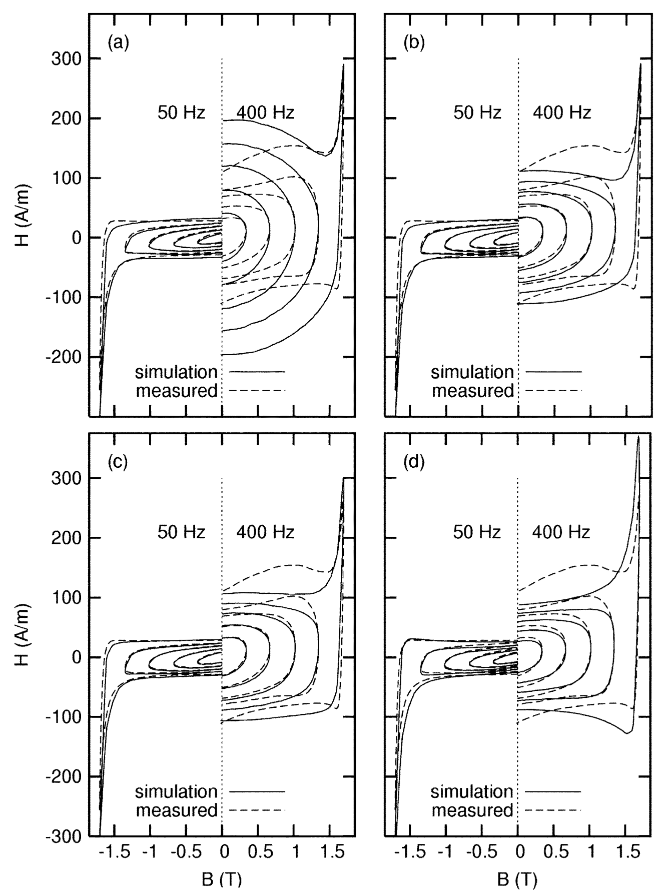

Fig. 2. Simulated and measured ac B–H loops: (a) $h_{\mathrm{EA}}(0), \gamma = 1$; (b) $h_{\mathrm{EA}}(0), \gamma = 0.75$; (c) $h_{\mathrm{EA}}(B), \gamma = 0.75$; (d) $h_{\mathrm{EB}}(B), \gamma = 0.75$.

The simulated loops at 400 Hz differ greatly from the measured ones because the ac hysteresis model (6) with (5) is too simple.

Next, the frequency dependence of $\gamma = 0.75$ is used. Fig. 3 shows the evaluation error of the total ac loss ($\int_{\mathrm{cycle}} H_{\mathrm{ac}} \mathrm{d}B$) given by $h_{\mathrm{EA}}(B, \mathrm{d}B/\mathrm{d}t)$ and $h_{\mathrm{EB}}(B, \mathrm{d}B/\mathrm{d}t)$ at 50 Hz. The error $\Delta\mathrm{loss}(\%)$ is given by the ratio of the discrepancy between the simulated and measured losses to the loss measured at a $B_{\max}$ of 1.7 T. To minimize the evaluation error at 50 Hz, this paper sets c_{A} for $h_{\mathrm{EA}}(B, \mathrm{d}B/\mathrm{d}t)$ and c_{B} for $h_{\mathrm{EB}}(B, \mathrm{d}B/\mathrm{d}t)$

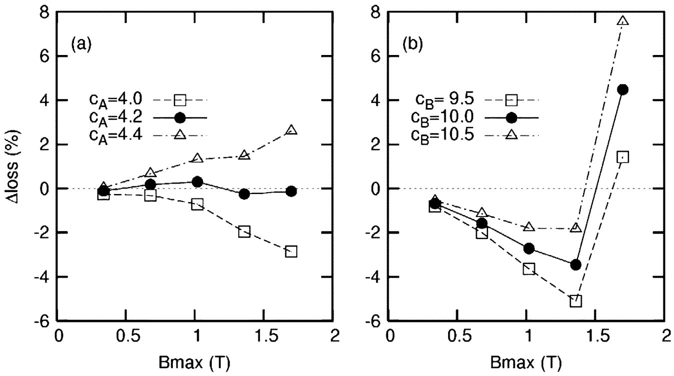

Fig. 3. Evaluation error of total ac loss at 50 Hz: (a) $h_{\mathrm{EA}}(B), \gamma = 0.75$; (b) $h_{\mathrm{EB}}(B), \gamma = 0.75$.

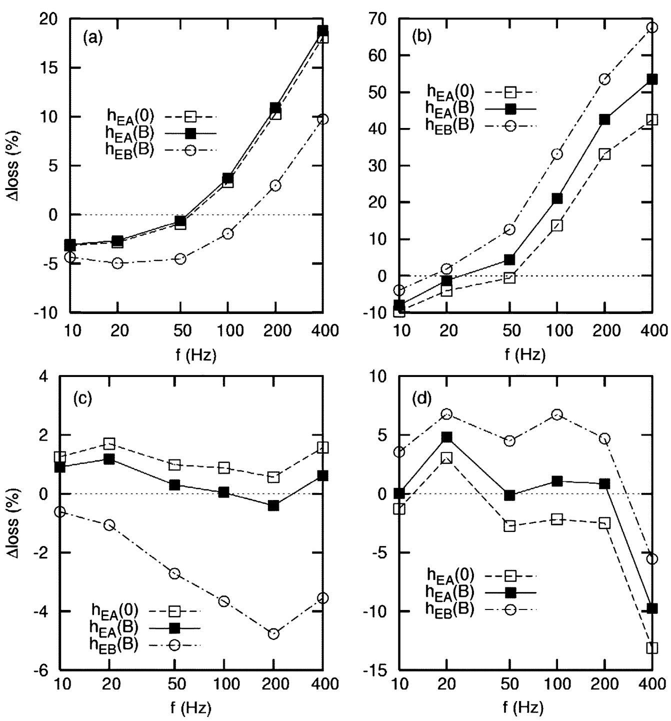

Fig. 4. Evaluation error of the total ac loss with $B_{\max}$ values of 1.02 and 1.7 T: (a) $\gamma = 1, B_{\max} = 1.02$ (T); (b) $\gamma = 1, B_{\max} = 1.7$ (T); (c) $\gamma = 0.75, B_{\max} = 1.02$ (T); (d) $\gamma = 0.75, B_{\max} = 1.7$ (T).

at 4.2 and 10.0 $(\mathrm{T/s})^{(1-\gamma)}$, respectively. Fig. 3 shows that $h_{\mathrm{EA}}(B, \mathrm{d}B/\mathrm{d}t)$ with a C_{A} of 4.2 $(\mathrm{T/s})^{0.25}$ gives a more accurate evaluation than $h_{\mathrm{EB}}(B, \mathrm{d}B/\mathrm{d}t)$.

Fig. 2(b)–(d) shows simulated B–H loops using $h_{\mathrm{EA}}(0, \mathrm{d}B/\mathrm{d}t), h_{\mathrm{EA}}(B, \mathrm{d}B/\mathrm{d}t)$, and $h_{\mathrm{EB}}(B, \mathrm{d}B/\mathrm{d}t)$, respectively, with γ = 0.75 and $L/d = 0.9$. The parameter c_{A} for $h_{\mathrm{EA}}(0, \mathrm{d}B/\mathrm{d}t)$ is set at 4.4 $(\mathrm{T/s})^{(1-\gamma)}$. Fig. 2 shows that a γ of 0.75 greatly improves the representation accuracy. Fig. 4 shows an evaluation error of the total ac loss for $B_{\max}$ of 1.02 and 1.7 T, while Fig. 5 shows the average discrepancy ΔH (A/m) between simulated and measured H with $\gamma = 0.75$. Fig. 4 shows that ac hysteresis models using $\gamma = 0.75$ accurately evaluate the ac loss. Figs. 2, 4, and 5 show that the field $h_{\mathrm{EA}}(B, \mathrm{d}B/\mathrm{d}t)$ seems to yield a slightly better representation than $h_{\mathrm{EA}}(0, \mathrm{d}B/\mathrm{d}t)$ and $h_{\mathrm{EB}}(B, \mathrm{d}B/\mathrm{d}t)$. However, simulated

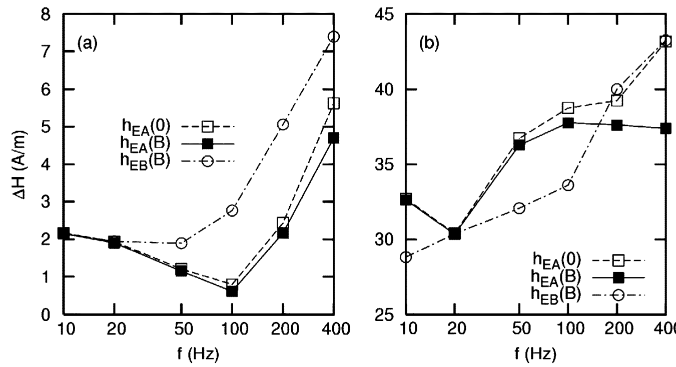

Fig. 5. Average discrepancy in H: (a) $\gamma = 0.75, B_{\max} = 1.02$ (T); (b) $\gamma = 0.75, B_{\max} = 1.7$ (T).

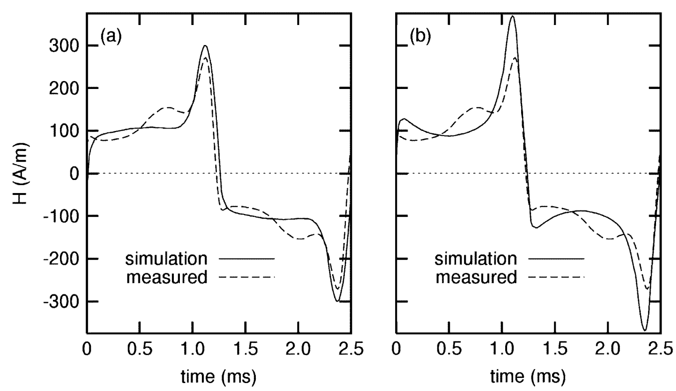

Fig. 6. Simulated and measured waveforms of H at 400 Hz: (a) $h_{\mathrm{EA}}(B), \gamma = 0.75$; (b) $h_{\mathrm{EB}}(B), \gamma = 0.75$.

B–H loops with an amplitude of 1.7 T at 400 Hz do not agree with the measured one in Fig. 2 because the models (10) and (11) are still too simple. For example, both $h_{\mathrm{EA}}(B, \mathrm{d}B/\mathrm{d}t)$ and $h_{\mathrm{EB}}(B, \mathrm{d}B/\mathrm{d}t)$ neglect the phase lag of H_{E} to $\mathrm{d}B/\mathrm{d}t$ caused by the skin effect. Fig. 6 shows waveforms of H given by $h_{\mathrm{EA}}(B, \mathrm{d}B/\mathrm{d}t)$ and $h_{\mathrm{EB}}(B, \mathrm{d}B/\mathrm{d}t)$ at 400 Hz with $\gamma = 0.75$. The phase discrepancy between the measured and simulated waveforms is seen in Fig. 6(b) for the case using $h_{\mathrm{EB}}(B, \mathrm{d}B/\mathrm{d}t)$. Fig. 6(b) also shows that $h_{\mathrm{EB}}(B, \mathrm{d}B/\mathrm{d}t)$ overestimates the maximum value of H.

IV. Simulation for Nonsinusoidal Magnetic Flux Density

This section compares simulated and measured ac hysteretic loops for the nonsinusoidal waveforms of B. Two input waveforms of B, shown in Fig. 7, are used to measure the minor loops of the grain-oriented silicon steel sheet. Inputs 1 and 2 contain third-order and 25th-order harmonics, respectively.

Fig. 8 shows simulated B–H loops for Inputs 1 and 2. It also lists the evaluation error of the total ac loss, $\Delta\mathrm{loss}(\%)$ and average discrepancy of $H, \Delta H$(A/m). Fig. 8 shows that the ac model with $\gamma = 1$ yields inaccurate B–H loops. The fields $h_{\mathrm{EA}}(B, \mathrm{d}B/\mathrm{d}t)$ and $h_{\mathrm{EB}}(B, \mathrm{d}B/\mathrm{d}t)$ with $\gamma = 0.75$ give accurate representations of the B–H loops. Fig. 8 also shows that a small $\Delta\mathrm{loss}$ does not always mean an accurate representation of a complex B–H loop.

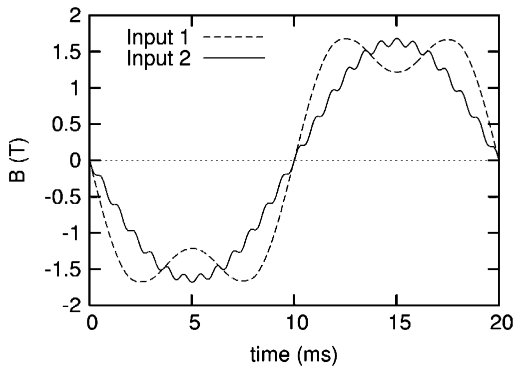

Fig. 7. Two input waveforms of magnetic flux density.

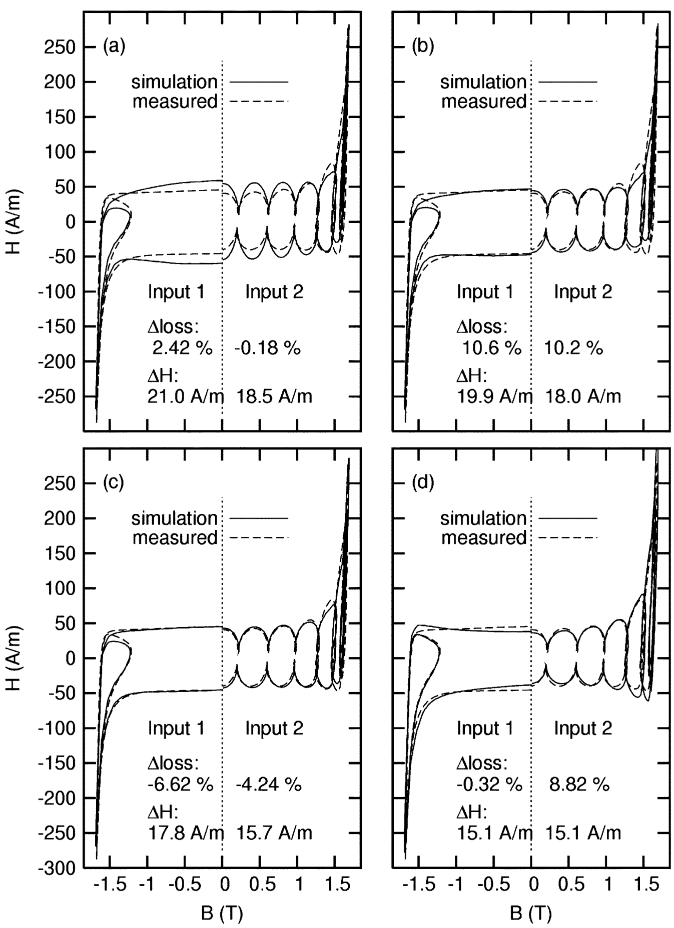

Fig. 8. Simulated and measured B–H loops having minor loops: (a) $h_{\rm EA}(0), \gamma = 1$; (b) $h_{\rm EA}(0), \gamma = 0.75$; (c) $h_{\rm EA}(B), \gamma = 0.75$; (d) $h_{\rm EB}(B), \gamma = 0.75$.

V. Conclusion

A simply generalized ac hysteresis model is proposed. It improves the evaluation accuracy of eddy-current loss and the representation of ac B–H loops under the condition of a sinusoidal magnetic flux. The generalized model also accurately represents ac B–H loops having minor loops. However, a further improvement in the ac model will be required to reduce the discrepancy between simulated and measured B–H loops for high frequency fields.

Acknowledgment

This work was supported in part by the Kansai Research Foundation for Technology Promotion and by a Grant-in-Aid for Scientific Research (C) (no. 16560243) from the Japan Society for the Promotion of Science.

References

[1] R. H. Pry and C. P. Bean, "Calculation of the energy loss in magnetic sheet materials using a domain model," *J. Appl. Phys.*, vol. 29, pp. 532–533, Mar. 1958.

[2] C. Kaido and T. Wakisaka, "Effect of material parameters on iron losses in nonoriented electrical steel sheets," *Trans. Inst. Elect. Eng. Jpn.*, vol. 117-A, pp. 685–690, Jul. 1997.

[3] G. Bertotti, *Hysteresis in Magnetism*. San Diego, CA: Academic, 1998.

[4] M. Enokizono, T. Todaka, S. Kanao, and J. Sievert, "Two-dimensional magnetic properties of silicon steel sheet subjected to a rotating field," *IEEE Trans. Magn.*, vol. 29, no. 6, pp. 3550–3552, Nov. 1993.

[5] M. A. Krasnosel'skii and A. V. Pokrovskii, *Systems with Hysteresis*. Berlin, Germany: Springer-Verlag, 1989.

[6] S. Bobbio, G. Miano, C. Serpico, and C. Visone, "Models of magnetic hysteresis based on play and stop hysterons," *IEEE Trans. Magn.*, vol. 33, no. 6, pp. 4417–4426, Nov. 1997.

[7] T. Matsuo, Y. Terada, and M. Shimasaki, "Stop model with input-dependent shape function and its identification methods," *IEEE Trans. Magn.*, vol. 40, no. 4, pp. 1776–1783, Jul. 2004.

[8] T. Matsuo and M. Shimasaki, "An identification method of play model with input-dependent shape fnction," *IEEE Trans. Magn.*, vol. 41, no. 10, pp. 3112–3114, Oct. 2005.

[9] T. Matsuo, Y. Terada, and M. Shimasaki, "Representation of minor hysteresis loops of a silicon steel sheet using stop and play models," *Physica B*, vol. 372, pp. 25–29, Feb. 2006.

[10] ——, "Representation of AC hysteretic characteristics of silicon steel sheet using simple excess eddy current loss approximation," *IEEE Trans. Magn.*, vol. 41, no. 5, pp. 1544–1547, May 2005.

[11] S. E. Zirka, Y. I. Moroz, P. Marketos, and A. J. Moses, "Dynamic hysteresis modeling," *Physica B*, vol. 343, pp. 90–95, 2004.

[12] T. Nakase, M. Nakano, K. Fujiwara, and N. Takahashi, "Method of digital waveform control for measuring magnetic properties by means of a single sheet tester," *Trans. Inst. Elect. Eng. Jpn.*, vol. 119-A, pp. 1019–1025, Jul. 1999.

Manuscript received June 20, 2005 (e-mail: tmatsuo@kuee.kyoto-u.ac.jp).